Journal of Unmanned System Technology

Flight Data Analyses of Fiber Optic Based Airworthy Structural Health Monitoring System for UAV using Artificial Neural Networks

Saransh Jain[†], Augustin M J[†], Kundan K Verma[†], Nitesh Gupta[†], Ramesh Sundaram[†], M Hariprasad[‡], and ACR Pillai[‡]

[†]Advanced Composites Division, CSIR-NAL, Bangalore, Karnataka, India

[‡]Aeronautical Development Establishment, DRDO, Bangalore, Karnataka, India

Abstract—This paper presents an airworthy, Fiber Bragg Gratings (FBG) based, Structural Health monitoring System (SHM) system for an Unmanned Aerial Vehicles (UAV). Various design issues pertaining to sensors location, embedment, integration of interrogation system instrumentation, online data recording, implementation of mathematical models for load estimations and GUI based flight data processing software are addressed. FBG data were processed to identify both vibration modes and loads using signal processing techniques and artificial neural network (ANN) algorithms respectively. The issue of sensor malfunctioning is also addressed wherein sensor failure was incorporated in the in-flight data during post processing for various flight regimes. The ANN based methodology was designed for identification of sensor failure and prediction of the estimated strain based on the available values from working (non-failed) sensors. The performance of load estimation was also compared in both the scenario (i.e. in the event of sensor failure and without sensor failure).

Keywords—Structural health monitoring, load estimation, algorithm development, artificial neural networks.

NOMENCLATURE

$\Delta\lambda_B/\lambda_B$	=	Shift in the reflected wavelength from the central wavelength of a free (not embedded) grating
ε	=	Mechanical strain along the local vicinity of the FBG sensor
ΔT	=	Temperature change
p_e	=	Effective strain-optic constant
α_Λ	=	Thermal expansion coefficient
α_n	=	Thermo-optic coefficient
$\alpha_{substrate}$	=	Thermal expansion coefficient of the composite substrate

I. INTRODUCTION

COMPOSITE materials are increasingly used as alternative to metals because of their excellent mechanical properties and manufacturability. In composite-made UAVs, SHM systems [1] should prove extremely important where conventional inspection methods of critical structural components are hindered by limited accessibility. Fiber optic sensors, in particular Fiber Bragg Grating sensors (FBG), appear to be excellent candidates to be used in SHM applications due to their high sensitivity to mechanical strain, excellent signal to noise ratio, large dynamic range, small size, immunity to electrical interference, low weight, long life and excellent durability under extreme environmental conditions. Moreover, multiplexing techniques have been devised; where quite a few sensors, longitudinally spaced on the same fiber, can be individually addressed to spatially cover strain and temperature fields. For composite structures, these sensors can be easily embedded during manufacturing, eliminating the need for sensor protection [2]. For example, a surface bonding FBG sensor net was successfully used for shape predictions of the doubly-tapered Ikhana wings during flight [3,4], taking advantage of the multiplexing capability of fiber optic sensors. Successful embedding technologies were also considered [5].

This work presents an advanced smart load monitoring airworthy system, for a UAV having composite tail booms. This is based on an array of FBG sensors, embedded in the tail booms during manufacturing. The system was tested on ground in order to verify its ability to track both static and dynamic boom loading. Structural characteristics like strain distribution under static loading, impact response, and normal modes were successfully traced by the system. Meaningful features (such as load) were extracted from the response of the structure during tests by implementing appropriate algorithms. In this study ANN is used as algorithm to estimate loads. The training data for these ANNs was provided by the tests conducted on the tail boom.

As a final proof of concept, the system was integrated in the Nishant UAV (designed & developed by ADE, India: **Figure 1**) and was successfully flown. The application of this technology will help in the reduction of direct operating and maintenance cost of the aircraft.

The issue of sensor malfunctioning is also addressed. In this study it is assumed that the malfunctioning FBG sensor does not give any output (zero value) during acquisition. This malfunctioning can be due to various reasons such as optical fiber breakage or optical power loss. The malfunctioning FBG is first identified and then the expected strain for that sensor is estimated using a separate set of ANNs.

Corresponding author: Nitesh Gupta (e-mail: ngupta@nal.res.in).
This paper was submitted on January 28, 2015; revised on May 14, 2015; and accepted on June 03, 2015.

Figure 1 Nishant UAV

II. FIBER BRAGG GRATING (FBG) SENSOR

The shift in the reflected wavelength from the central wavelength of a free (not embedded) grating, / , due to an applied strain along the fiber (ε) & change in temperature (ΔT) is approximately given by [2].

$$\frac{\Delta\lambda_B}{\lambda_B} = (1 - p_e)\,\varepsilon + (\alpha_\Lambda + \alpha_n)\,\Delta T \qquad (1)$$

Figure 2 shows working principle of FBG

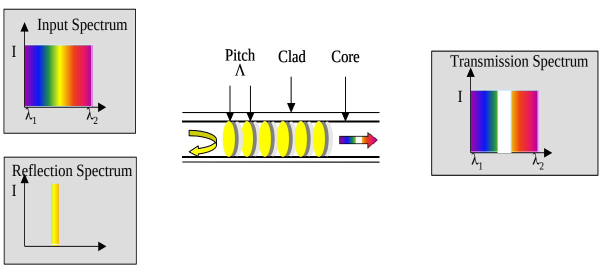

Figure 2 Working principle of FBG

An embedded fiber, firmly attached to its surrounding matrix, is also affected by the thermally induced mechanical strains in that composite substrate. Therefore, for an embedded fiber, where the transverse mechanical coupling between the fiber & the composite substrate is small, Equation (1) should be rewritten as:

$$\frac{\Delta\lambda_B}{\lambda_B} = (1 - p_e)\,\varepsilon + (\alpha_\Lambda + \alpha_n)\Delta T + (1 - p_e)(\alpha_{substrate} - \alpha_\Lambda)\Delta T \qquad (2)$$

As the UAV experiences temperature changes during flight, it is necessary to compensate for the temperature induced $\Delta\lambda_B/\lambda_B$ in order to get the true mechanical strains. Boom heating test was conducted in order to evaluate the total thermal effect on the embedded Bragg grating sensor wavelength shift. The procedure of removing the thermal effect will be discussed further. True structural strain values were used for the development of Artificial Neural Network based boom load estimation.

III. ARTIFICIAL NEURAL NETWORKS

ANN is a mathematical model or a computational model that is inspired by the structure and/or functional aspects of biological neural networks. A neural network consists of an interconnected group of artificial neurons. Implementation of ANN is a 2 step process. In the first step, the network is trained using known input and output data. Once trained, the network can be used for prediction of a new input, which was not used for training (**Figure 3**).

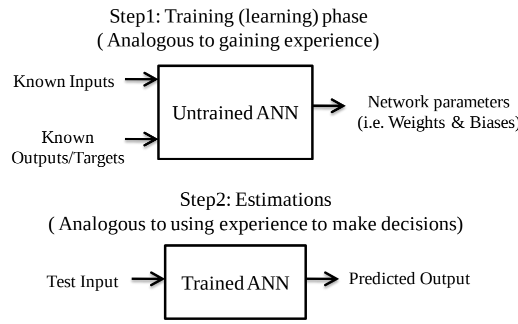

Figure 3 Philosophy of ANN

ANNs can be trained to perform a particular function. Theses trained ANNs then can be used to make estimations (such as load or damage estimations).

IV. SENSOR LOCATION IDENTIFICATION AND EMBEDMENT

The NishantUAV, designed and manufactured in India by ADE. Nishant UAV has two composite tail booms, made of two thin wall "C" section channels, riveted together to form a close rectangular beam. These booms hold the empennage (comprising a horizontal tail with elevator and two vertical tails). The thickness of the composite boom walls is optimized for both strength and stiffness [6].

The boom is essentially a cantilever beam with a relatively large mass at the back end. Vertical and horizontal bending are the main boom loading conditions. **Figure 4** shows a typical layout of the FBG sensors in a C-section along with boom cross section. The two centre fibers are only sensitive to the vertical bending. The side fibers are sensitive to the vertical bending in a similar manner as the central ones, but will also react to horizontal bending. The vertical bending introduces similar but opposite strains in the top and bottom fibers. The two side fibers are on the same side with respect to the center line. Hence, the horizontal bending induces similar strains on both side fibers, in addition to the vertical bending contribution.

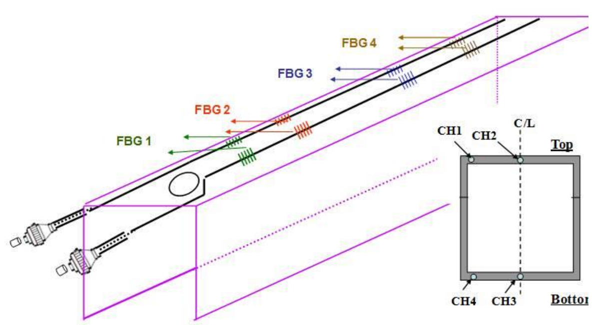

Figure 4 Embedded optical fibers locations and general boom layout

A patch embedment concept was developed in this study in order to protect the fibers during the production and assembly process. Additional composite layers were added on top of the patch, yielding a protected embedded sensor net ensuring the structural integrity and efficiency of the embedment process in terms of boom manufacturing time.

V. Instrumentation and Ground Level Tests

The airworthy SHM instrumentation consists of an FBG interrogator, on-board computer, battery, electrical & fiber optic interconnects and mounting fixtures. A solid state, high sampling rate (>2 KHz) FBG interrogator capable of reading multiple FBGs simultaneously, distributed across four fibers (4-channles) was used. Measured data was transferred over an Ethernet cable to an on-board computer, which can control the interrogator and also store the data on a solid state drive. The complete assembly of these units was placed in the payload bay of the UAV on a specially designed mounting fixture. These instruments was tested & verified for their functionality, as per the Environmental Screening Specification (ESS) requirements of the UAV comprising vibrations, shock and temperature tests.

Ground tests consists of (a) Static & dynamic testing of boom & (b) Ground engine run tests with boom assembled onto UAV, with above SHM instrumentation. The sensor data obtained from static testing were also compared with the FEA data.

Static testing of booms was carried out to correlate embedded FBG readings with collocated surface bonded strain gauges for different load cases. **Figure 5** shows the typical static test setup.

Figure 5 Experimental setup for boom static testing

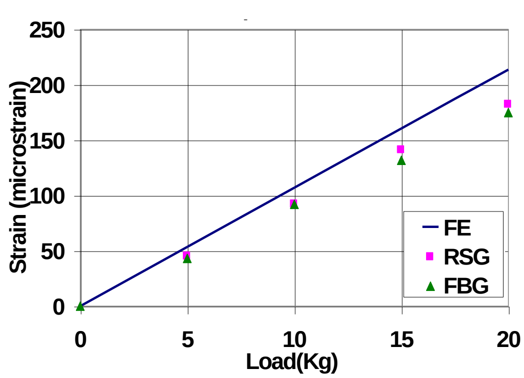

Figure 6 Static test results

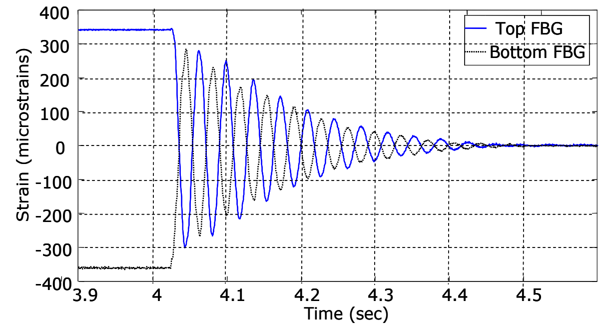

Figure 7 Dynamic test data

Figure 6 shows the response of the FBG & strain gauges at various load values for a typical sensor location on boom. From the plots it can be observed that the strain gauge & FBG data are in good agreement with FEA values.

Several tests were performed to evaluate the ability of the embedded sensor to track the dynamic behavior of the boom [7]. In this work, at the boom end a weight of 60 kg was attached and released by cutting its attachment to the boom. The FBG readings during the dynamic test are shown in **Figure 7**. The first bending mode frequency of the cantilever boom obtained by the Fourier analysis of the dynamic test data was 27.6 Hz.

Based on several ground tests the feasibility of SHM system of detecting small strains was proved and the instrumentation was cleared for flight trail.

VI. Flight Test & Flight Data Analysis

The Nishant UAV equipped with above airworthy SHM system was flown at Kolar Airfield near Bangalore, India. It was demonstrated that the system captured the data successfully from all 16 FBG sensors of the 4 center fibers of both booms, starting from launch, flight maneuvers & parachute recovery.

The first step in the evaluation of the mechanical behavior of the booms is to isolate the temperature induced strains. This was achieved using push-pull topology which takes into account the readings from sensors embedded in top and bottom C sections of the boom. Adding the top and bottom strains of each center fiber FBG sensors pairs isolate the temperature effect, (**Figure 8**). Once FBG readings are acquired, this sensor arrangement enables direct identification of the two bending loads on each boom. The center boom sensors, embedded in pairs into the top and bottom skins, at the same distance from the boom end, react very similarly to temperature changes, but oppositely to vertical bending. By adding these two readings the mechanical loading effect is canceled and the temperature contribution on the FBG readings can be evaluated. Additional low pass filter of 0-35Hz was also applied to remove frequencies associated with noise and higher skin bending (local) modes. The temperature effect, as obtained from the sensors was compared to the flight elevation data, translated to FBG readings using the standard temperature-altitude profile combined with the embedded FBG CTE obtained during ground heating test.

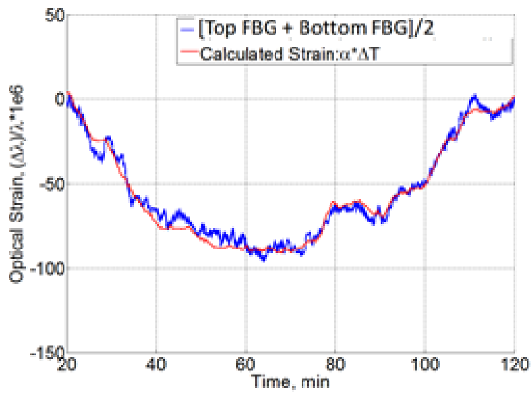

Figure 8 Raw FBG readings during flight, showing the combined effect of strain and temperature (thicker-blue curve). Superimposed is a curve of the effect of temperature alone based on the UAV height, as obtained from telemetry.

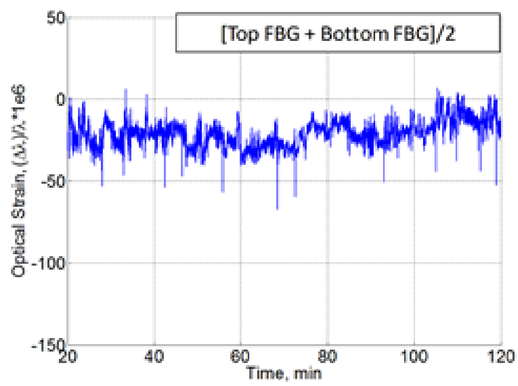

Figure 9 Boom loads and vibration signature after removal of temperature effect

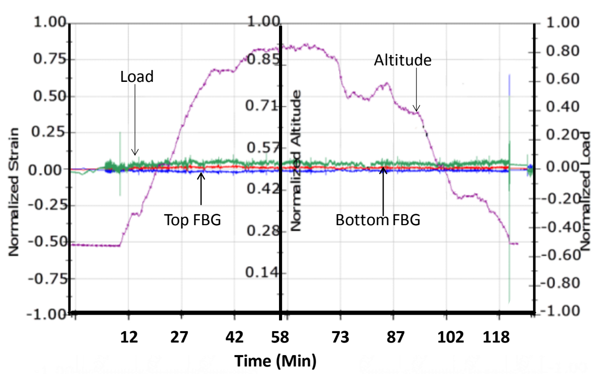

Figure 10 Complete flight profiles

The boom vibration signature, excluding launch and landing, can be seen in **Figure 9**. The temperature compensated strain values for top & bottom sensors for complete flight profile is shown in **Figure 10**, whereas for launch and recovery its shown in **Figure 11** and **12** respectively. It is observed from the plot that the readings of the sensors are out of phase as they are located on top & bottom center fibers of the composite boom structure.

The basic concept for tracking the structural integrity of the booms is based on cross correlation between normalized sensors. Since the boom itself is light with respect to the weight of the horizontal and vertical tails, the first vibrational bending mode is dominant. This is especially valid for the case of ground touch-down impact during UAV landing.

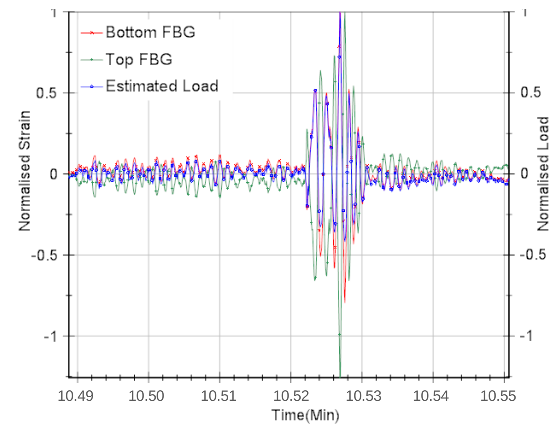

Figure 11 Temperature compensated strain & ANN estimated load during launch

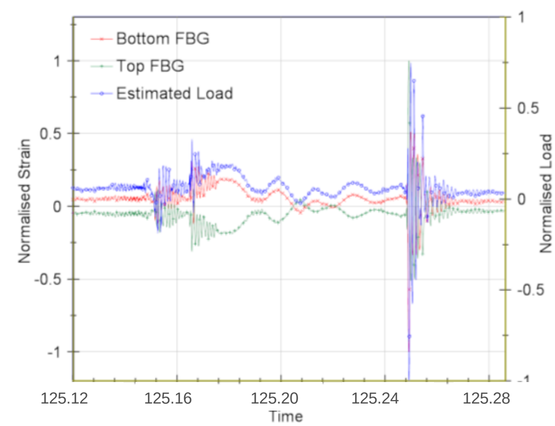

Figure 12 Temperature compensated strain & ANN estimated load during recovery

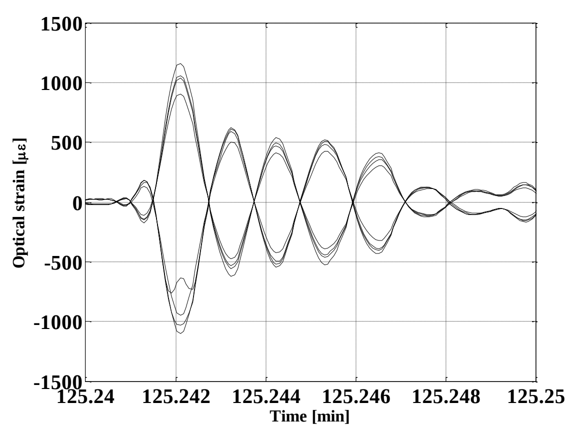

Figure 13 FBG readings during landing

The most critical loading condition during the Nishant UAV test flight is its landing, especially the ground touch-down. This research tracks events during landing which is associated with high loads and evaluates occurrence of damage, if any, during such events. **Figure 13** shows FBG reading during landing. It is clear from the figure that top and bottom FBG strains are out of phase because of bending. There is slight glitch in one of the top FBGs (with negative strains) which represent occurrence of an unexpected event (such as local buckling in the boom).

The analysis of the sensor data and subsequent processing with various signal processing tools and algorithms is an important part of Structural Health Monitoring. QUICKVIEW is software developed in National Aerospace Laboratories, Bangalore, India to have an immediate look on the sensor data recorded by the SHM system in UAVs during its operation. This software enables the quick view of sensor data during the flight, which is not possible in conventional way due to its large size (~6 GB for two and half hours). The representation of the in-flight sensor data along with flight parameters will provide information about strain and load during various maneuvers. The other key features of the software are – Modular design which enables further modification and expansion easy, powerful graphical user interfaces which allows separate views of a 3 D model of the aircraft simulate the flight manures, Strain view for all the sensors, estimated load view. The ANN objects developed in Matlab are embedded called in the code for the faster estimations. Provisions are made in the software to down sample the data and save a portion of the file of smaller size to do detailed processing. Screenshots of various tabs of the software are shown in **Figure 14, 15** and **16**.

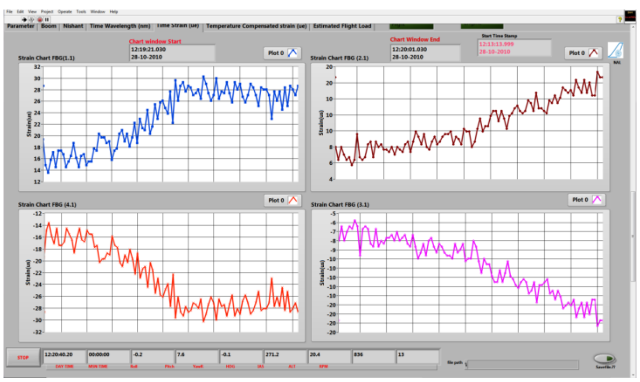

Figure 14 StrainVIEW tab

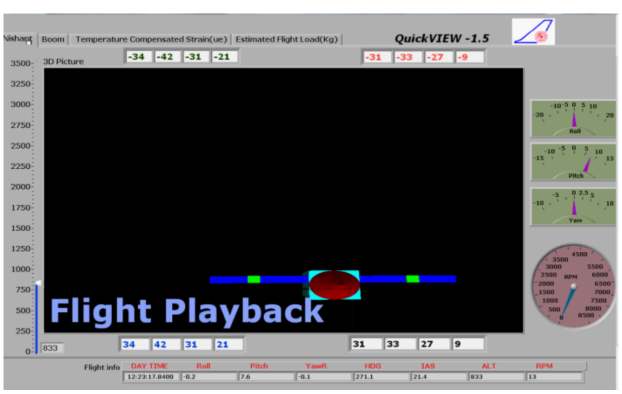

Figure 15 Flight VIEW tab

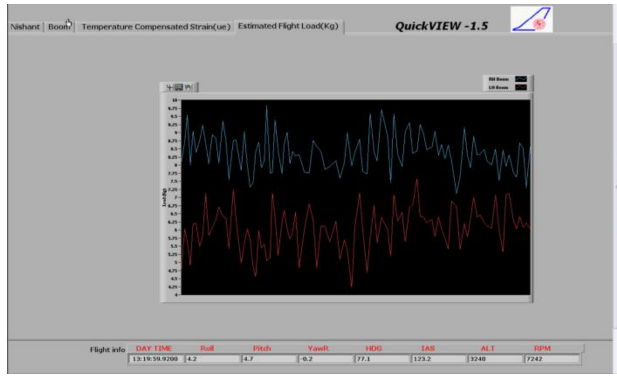

Figure 16 ANN estimated load VIEW tab

VII. Artificial Neural Network (ANN) Based Load Estimator

The sensor data acquired during flight need to be converted into meaningful information (e.g. load or damage). ANN based techniques were employed [1,8,9] to process the sensor data and provide substantive information about the structure. ANNs are data driven mathematical models. They are usually required when a specific equation or algorithm is not applicable, but when adequate knowledge or database exist (either from experiments or analysis or both) to derive knowledge based solutions [10].

In this research, a 2 layer feed-forward back propagation ANN based load estimator was developed. The hidden layer comprises 16 neurons and the output layer has 1 neuron. All neurons in the hidden layer have “sigmoid” transfer/activation function while the neuron in output layer has “linear” transfer/activation function. The strain patterns across individual booms from center fiber FBGs were used as inputs & corresponding bending load values were used as the targets for training of the network.

In order to estimate the flight loads, the temperature compensated strain values as determined in the previous section, were used. These strain patterns were given as inputs to the trained load estimator. The output of the estimator was the predicted flight loads. The estimated load values for complete flight profile (**Figure 10**), launch (**Figure 11**) & recovery phase (**Figure 12**) of UAV are shown.

VIII. Sensor Malfunctioning

Sensor malfunctioning is one of the major issues during experiments, testing or even in on board sensors. The data measured through sensors is subsequently used for processing and estimations. A malfunctioned sensor would either give no value or an irrelevant value. Estimations based on this data could be erroneous. In the context of FBG sensors, malfunctioning can happen because of various reasons such as improper bonding, optical fiber breakage, mishandling of sensors etc. In this work, an ANN based load estimator is implemented. This network utilizes data measured from 16 FBG strain sensors to make estimations. Malfunctioning of one or more FBGs directly affects the accuracy of load estimations. In this study issue of sensor malfunctioning is addressed assuming that the fiber has been broken thereby FBG reading during the measurement goes to zero. Based on this zero strain over a period of time, the malfunctioning sensor is identified. For this malfunctioning sensor the intended strain (strain which it would have measured if it was not malfunctioning) is computed using strains of rest of the working sensors. To resolve this issue, a set of 16 ANNs is implemented, one ANN for each sensor. These 16 networks are collectively termed as ANN_MFSE. Once a malfunctioning FBG sensor is identified, ANN_MFSE takes the strains measured by the remaining 15 sensors as input to predict the strain at the malfunctioning sensor location. The estimated strain replaces the zero strain and the modified strain vector is fed to the load estimator. This scheme is shown in **Figure 17**.

Each ANN_MFSE network is a 2-layer feed-forward back-propagation network with 20 neurons in the hidden layer and 1 neuron in the output layer. All neurons in the hidden layer have "sigmoid" transfer/activation function while the neuron in output layer has "linear" transfer/activation function. The format of training data for ANN_MFSE is shown in **TABLE I**. In this example, the sensor S4 is considered as malfunctioning. Similar training data exists for the other 15 networks as well and each network is trained with its corresponding training data.

Performance of ANN_MFSE was evaluated based on a test case in which it is assumed that sensor S4 malfunctions and gives zero strains as output. Here two cases were considered. In the first case, the input vector (containing zero strain from malfunctioning sensor) was directly fed to the load estimator (based on ANN) for estimating load. In the second case, the input vector was first fed to ANN_MFSE which estimated the expected strain for sensor S4. The comparison of estimated strains with original strains (as acquired during flight) is shown in **Figures 18** and **19**. This estimated strain replaced the zero strain in the input vector and this modified inputvector was then fed to the load estimator based on ANN. Comparison of estimations for these two cases along with expected outputs are plotted in **Figures 20**.

TABLE II presents the comparison of error (Root mean square error - RMSE) between estimations with and without implementation of ANN_MFSE.

TABLE III shows the estimations of maximum load during the flight in the both the cases i.e. with and without ANN-MFSE. Finally, **TABLE IV** presents the absolute error in estimation of maximum load for the same cases. **Figure 18** and **Figure 19** show that ANN_MFSE can estimate strains for malfunctioning sensors with significant accuracy. The accurate estimations of strains further aid in improved load estimations.

TABLE II depicts appreciable reduction in root mean square error when neural networks are used for strain estimations of malfunctioned sensor.

TABLE III and **TABLE IV** show that there is substantial reduction in absolute error in the estimations of maximum loads when ANN_MFSE is used. **Figure 20** along with **TABLE II**, **TABLE III** and **TABLE IV** shows that, in case of sensor malfunction, load estimations can be improved appreciably if the process is integrated with ANN_MFSE.

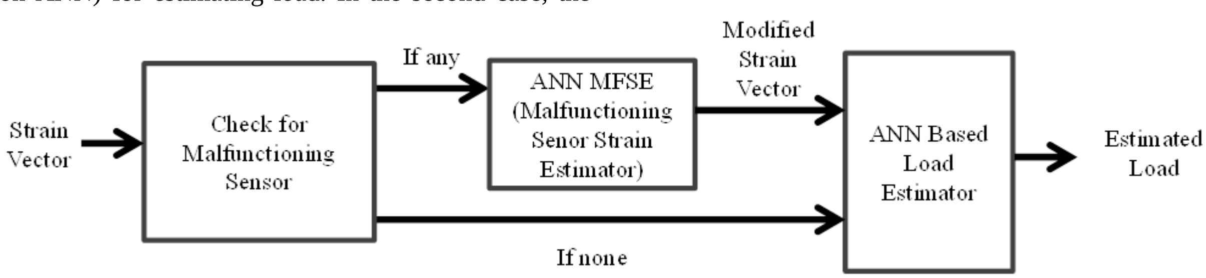

Figure 17 Complete estimation process including ANN MFSE

Table 1 Training data format for ANN_MFSE

S.No.	S1	S2	S3	S4	S5	.	.	.	S16
1	-46.513	-70.531	-65.886	-62.849	-58.312				62.849
2	-42.012	-68.302	-65.57	-61.29	-57.026				61.29
.									
.									
1188	-67.399	-32.632	-13.708	-15.434	-4.323				15.434
1189	-82.513	-24.032	-14.025	-19.178	-4.323				19.178
	-------------------Inputs------------------			Targets	-------------Inputs-------------				

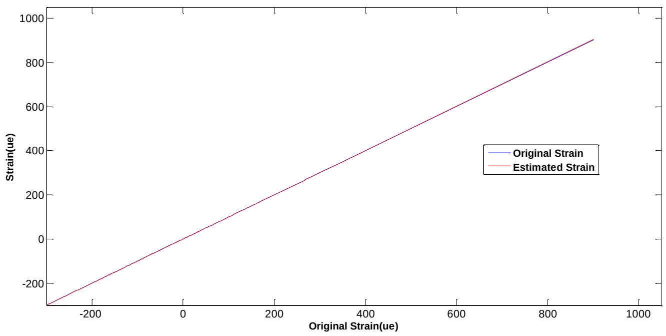

Figure 18 Comparison of original strains with estimated strains using ANN

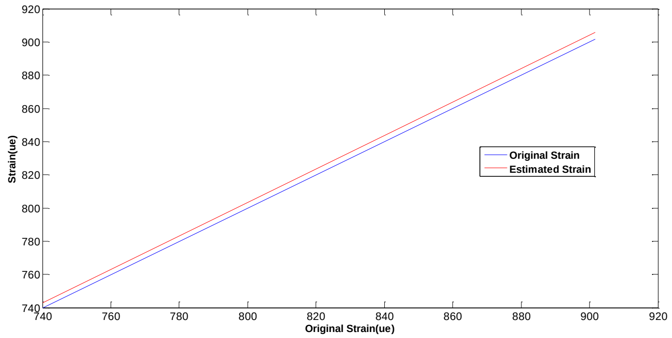

Figure 19 Comparison of original strains with estimated strains using ANN

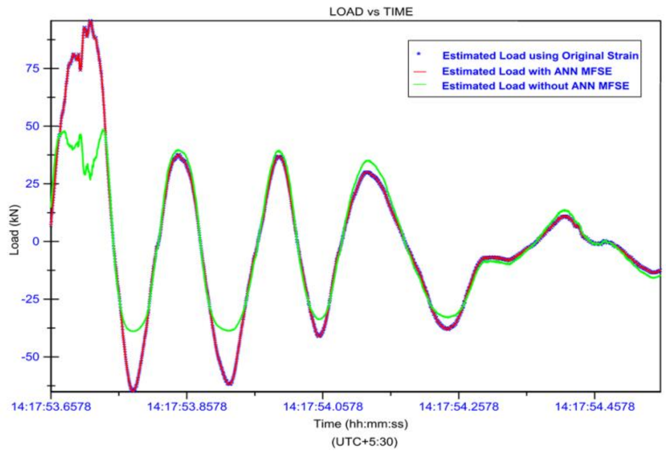

Figure 20 Comparisons of estimated loads

TABLE II COMPARISON OF ERRORS WITH AND WITHOUT IMPLEMENTATION OF ANN_MFSE

RMSE using Neural Networks for strain estimation	RMSE without Neural Networks strain estimation	Number of data points used for estimations
0.0307	12.7814	2243

TABLE III COMPARISON OF MAXIMUM LOAD ESTIMATIONS WITH AND WITHOUT IMPLEMENTATION OF ANN_MFSE

Original load	Load estimation using ANN MFSE	Load estimation without ANN MFSE	No of data points used for estimations
95.7023	95.6277	27.5431	2243

TABLE IV COMPARISON OF MAXIMUM ABSOLUTE ERRORS IN LOAD ESTIMATIONS WITH AND WITHOUT IMPLEMENTATION OF ANN_MFSE

Maximum error in load estimation without ANN MFSE	Maximum error in load estimation with ANN MFSE
68.8737	0.2146

IX. CONCLUSIONS & FUTURE WORK

An airworthy, FBG based SHM system was developed. A successful flight trial was completed with this system on Nishant UAV. Rugged sensor embedment schemes were implemented. Software to handle large amount of data acquire during the flight was developed. The instrumentation scheme was developed for the harsh operating conditions of the UAV. A load estimator based on ANN was implemented and the loads were estimated at different flight regimes (i.e. take off, engine start, cruise, land). Furthermore, a methodology to estimate strains for sensor malfunction was developed. ANN based estimators were used to identify and estimate the expected strains of malfunctioning sensors. The future work should include the problem of addressing multiple sensor failures simultaneously.

ACKNOWLEDGMENT

Authors are thankful to Mr. HN Sudheendra, Head, ACD, Dr. Byji Varghese, Mr. Kotresh M Gaddikeri, Mr. HV Ramchandra, Mr. B. Ramanaiah, Mr. Gururaj KM, Mr. Amith&Ms V DeepuBai of NAL for their help during the course of work. Authors express their sincere thanks to Prof. Tur from Tel-Aviv Univeristy and Mr. IddoKressel from IAI, Israel, Mr. G Natarajan, Mr. G Siva Sankaran, Mr. G Sreenivasa Murthy from ADE for their help and thoughtful suggestions. Authors are grateful to Dr. AR Upadhya, former director NAL & Mr. PS Krishnan, Director ADE for their encouragement & support. Authors finally thank Mr. ShyamChetty, Director NAL for his unstinted support.

REFERENCES

[1] WJ Staszewski, C. Boller and G.R Tomlinson, Health Monitoring of Aerospace Structures, John Wiley & Sons, 2004
[2] Andreas, O., and Kyriacos, K., Fiber Bragg Grating. Fundamentals and Applications in Telecommunications and Sensing, Artech House, 1999.

[3] William L. Ko, W. L. Richards, and Van T. Tran, “Displacement Theories for In-Flight Deformed Shape Predictions of Aerospace Structures,” NASA report TP-2007-214612, 2007.

[4] William L. Ko, W Lance Richards, and Van Tran Fleischer, “Applications of Ko Displacement Theory to the Deformed Shape Predictions of the Doubly-Tapered Ikhana Wing,” NASA report TP-2009-214652, 2009. CrossRef

[5] Sundaram, R., et.al. , “Structural health monitoring of co-cured composite structures using FBG sensors,” Proceedings of SPIE International Conference on Smart Structures & Systems, Newport, USA, 2005.

[6] M. Tur, et.al. , “The use of optical fiber sensors for load tracking & structural health monitoring of UAV composite structures,” ICAUV, Bangalore, India, 2009.

[7] A Handelman, et.al. , “Load tracking & structural health monitoring of Unmanned Aerial Vehicles using optical fiber sensors, ” 10th International Conference on Fiber Optics and Photonics, IIT Guwahati, India, 2010. CrossRef

[8] Chang, F.-K. and Beard, S., “Active damage detection in filament wound composite tubes using built-in sensors and actuators,” Journal of Intelligent Material, Systems and Structures, 8: 891-897, 1997. CrossRef

[9] Staszewski, W.J., Read, I. and Foote, P., “Damage detection in composite materials using optical fibres– recent advances in signal processing,” Proceedings of the SPIE’s 7th International Symposium on Smart Structures and Materials, Conference on Smart Structures and Integrated Systems, Newport Beach, California, 2000.

[10] Kamath, G.M. et.al. , “A neural network based health monitoring methodology for co-cured/ co-bonded composite aircraft structures,” Proceedings of the 3rd European Workshop on Structural Health Monitoring, Granada, Spain, 2006.